Optimal Design of Piezoactuators for Active Noise and Vibration Control

S. J. Kim* and J. D. Jones†
Purdue University, West Lafayette, Indiana 47907

A generalized approach for the optimization of piezoactuator/substructure coupling for active noise and vibration control is studied. The effective bending moment induced by twin, rectangularly shaped piezoactuators surface-bonded to the upper and lower surfaces of a thin, flat plate is estimated from a static analysis of the composite structure. For the degenerate case of zero bonding layer (i.e., perfect bonding), the effective bending moment obtained from this study is compared with pre-existing methods. The optimal thickness of piezoactuators that maximize the effective moment under a constant electric field is estimated. This study shows that the optimal thickness of the piezoactuators approaches half the thickness of the plate (assuming a steel plate). The influence of Young's modulus of the piezoactuators, the bonding layer thickness, and the damping and material properties of the bonding layer on the optimal thickness of the piezoactuators is also presented. An increase in the Young's modulus of the piezoactuators reduces the optimal thickness of the actuators, and gives larger bending moments. The thickness of the bonding layer does not significantly affect the optimal thickness of the piezoactuators; however, thicker bonding layers give lower bending moments. Finally, the damping and material properties of commercially available bonding materials do not significantly influence either the optimal thickness of the piezoactuators or the induced bending moment, given the bonding layer is thin with respect to the composite thickness.

Nomenclature

d_{31} = piezoelectric strain constant, m/V or C/N
E = Young's modulus, N/m^2
E_{mf} = maximum allowable electric field strength, V/mm, Table 1
h = one-half plate thickness, mm
m = effective bending moment, N-m/m
t = thickness, mm
V = applied voltage, volt
x, y, z = rectangular coordinates, centered on the plate neutral axis
α = nondimensional bonding layer material property ratio, Eq. 14
β = nondimensional piezoactuator material property ratio, Eq. 14
γ = piezoactuator stress-strain ratio, Eq. 14
Δ = strain slope, (m/m)/m, Eq. 7
ε = strain, m/m
η = damping factor, Fig. 8
Λ = free piezoelectric strain, m/m, Eq. 10
ν = Poisson's ratio
ρ = nondimensional thickness ratio, mm/mm, Eqs. 16 and 17
σ = stress, N/m^2

Subscripts

b = bonding layer
il = plate/bonding layer interface
p = plate
x = x direction
y = y direction
z = piezoactuator

Superscript

c = complex

Presented as Paper 90-3925 at the AIAA 13th Aeroacoustics Conference, Tallahassee, FL, Oct. 22-24, 1990; received Nov. 9, 1990; revision received June 5, 1991; accepted for publication June 6, 1991.

*Graduate Student, School of Mechanical Engineering, Ray W. Herrick Laboratories.

†Associate Professor, School of Mechanical Engineering, Ray W. Herrick Laboratories.

Introduction

PIEZOELECTRIC materials exhibit an interesting phenomenon, whereby upon mechanical strain a measurable electric polarization (or voltage) proportional to the strain is produced. As such, piezoelectric materials have found common use in sensing devices such as accelerometers. However, piezoelectric materials also exhibit an inverse effect, whereby an applied voltage across the material induces a mechanical strain in the material and thus can be used as an actuator device. With the development of fine ceramic technology, piezoelectric transducers have found widespread use in a diverse range of innovative applications including surface acoustic wave (SAW) filters, micropositioning controllers, ultrasonic motors, and frequency analyzers.

In recent years, much research effort has been devoted to developing active noise and vibration control techniques using piezoelectric actuators and sensors. Piezoelectric transducers have shown great promise for use as distributed actuators and sensors because they are inexpensive, space efficient, lightweight, and are easily shaped and bonded to (or embedded in) a variety of surfaces. Also, the distributed nature of piezoactuators can be used to provide control with a minimum of control spillover. Furthermore, in contrast to conventional point actuators, piezoactuators do not require a back reaction.

Bailey and Hubbard[1] explored the possibility of using piezoelectric actuators as active dampers for one-dimensional beams. Substantially reduced vibrational decay times were demonstrated using the piezoelectric dampers. Fansen and Chen[2] and Baz and Poh[3] also presented significant research works on the use of piezoelectric dampers for active control of the one-dimensional beam problem. The potential of piezoactuators was again demonstrated by these investigators showing that a number of vibrational modes can be simultaneously controlled with reduced spillover of energy into higher order modes.

Crawley and de Luis[4] presented a rigorous study of the stress-strain-voltage behavior of twin, symmetric surface-bonded

and embedded piezoactuators in one-dimensional cantilever beams. Several important results were demonstrated including the increased piezoactuator/beam coupling for stiffer and thinner bonding layers and stiffer piezoelectric materials. Crawley and de Luis also demonstrated that the shear stresses at the bonding layer/beam interface become uniform within the actuator boundaries when the bonding layer is assumed infinitely thin (i.e., the actuator is perfectly bonded).

Recently, Dimitriadis and Fuller[5,6] investigated the behavior of a pair of two-dimensional piezoelectric patches surface-bonded to an elastic plate and used as distributed vibration actuators. This investigation is a two-dimensional extension of Crawley's work.[4] However, there were some distinguishing differences in the fundamental assumptions which are discussed in the following section of the current study. It was demonstrated that modes can be selectively excited and that the geometry of the actuator shape markedly affects the modal distribution of plate. The location of the piezoactuator was similarly shown to affect dramatically the vibration response of plate. Furthermore, the analysis was extended to accommodate the use of piezoactuators for active noise control of structurally radiated/transmitted noise.[6] Again, piezoactuators demonstrated great potential in controlling structurally radiated/transmitted sound.

In the current work, a generalized approach to the optimal design of a piezoactuator for active vibration control of an elastic plate is presented. An effective moment expression is developed from a static analysis of the composite structure. The analysis also includes a comparison with two existing methods: one from Dimitriadis's work[5] and the other from a two-dimensional extension of Crawley's work.[4] The optimal thickness of a piezoactuator under a constant electric field is estimated. In addition, the influence of the thickness, damping, and material properties of the bonding layer on the effective moment and optimal thickness of the piezoactuator is presented. Finally, the effects of Young's modulus of the piezoactuators and the bonding layer are also discussed.

Piezoactuator/Substructure Coupling Analysis

A free (i.e., unconstrained) piezoelement (assumed to be a ferroelectric ceramics and polarized along the z direction in this study) simultaneously develops compressive or tensional strain in the x, y, and z directions when activated by applying a voltage across z direction. The induced strains for each direction are determined by the sign and amplitude of the applied voltage and the piezoelectric strain constants of the material. As polarized ferroelectric ceramics effectively have the symmetry of a hexagonal crystal in class $C_{6v} = 6\,\text{mm}$,[7] the free strains in x and y direction are equal.

When piezoactuators (symmetrically bonded to the upper and lower surface of a plate) are activated, surface tractions proportional to the magnitude of the applied voltage are generated at the piezoactuator/plate interfaces. The direction of the tractions are determined by the poling direction of the piezoactuators and the sign of the applied voltage. If both actuators are arranged to generate surface tractions of equal sign, the plate will experience surface extraction or contraction forces (in-plane membrane forces). When both actuators are arranged to generate surface tractions of opposite sign, the plate will then experience bending forces. If the applied voltage varies sinusoidally with time, the plate experiences harmonic excitation. Since the plate bending vibration is generally more important than the plate membrane vibration in low-frequency noise and vibration control problems suitable for active control, the configuration of the actuators and the applied voltages are assumed to generate exclusively bending forces in this study.

Review of Previous Studies

Crawley and de Luis[4] developed a rigorous analysis of the piezoactuator/substructure coupling for a one-dimensional beam. In the analysis, several important assumptions were made, including linear strain variation across the beam thickness, uniform strain across the piezoactuator, and a shear stress carrying viscoelastic bonding layer for the surface bending configuration of the piezoactuators (see Fig. 1a). The surface shear stresses at the beam/bonding layer interfacing surfaces were obtained from a static analysis of the beam and showed that the shear stresses become uniform along the piezoactuator length when the bonding layer becomes infinitely thin. It was also shown that stiffer piezoactuators provide higher bending moments. Uniform strain across the piezoactuator implies that the piezoactuator will not bend. Under this assumption, the deflection behavior of the composite structure (shown greatly exaggerated in Fig. 1b) is not generally plausible. However, this model is valid for the relatively thin piezoactuators, where the thickness of piezoactuator is small in comparison to the substructure thickness.

Dimitriadis and Fuller[5] extended the application of piezoactuators to the plate vibration control problem. Under the assumptions of zero bonding layer thickness (perfect bonding) and linear strain variation across the combined structure thickness, a relationship for the effective bending moments exerted on the plate by the piezoactuators was derived. It was shown that the effect of the piezoactuator patch was to create a uniform surface moment within the boundaries of the piezoactuator. Thus, the effect of the piezoactuator is equivalent to a constant edge moment around the boundaries of the patch. In the analysis, it was also assumed that the plate and piezoactuators have identical stress slopes, as shown in Fig. 2. However, unless both the piezoactuator and plate layers have identical elastic properties, the stress slopes for each layer should, in general, be different, given a linear strain distribution across the composite structure. Nevertheless, this work is an important contribution from the perspective that the potential use of piezoactuators was proven for the two-dimensional plate vibration problem.

Derivation of the Effective Moment

In this section, a new derivation for the effective moment induced by the twin piezoactuators surface-bonded to an elastic plate is presented. The analysis follows closely that of Dimitriadis and Fuller.[5] However, differences in fundamental assumptions distinguish this analysis from previous studies.

Given a combined structure that is thin compared with radius of curvature, a linear strain distribution can be assumed

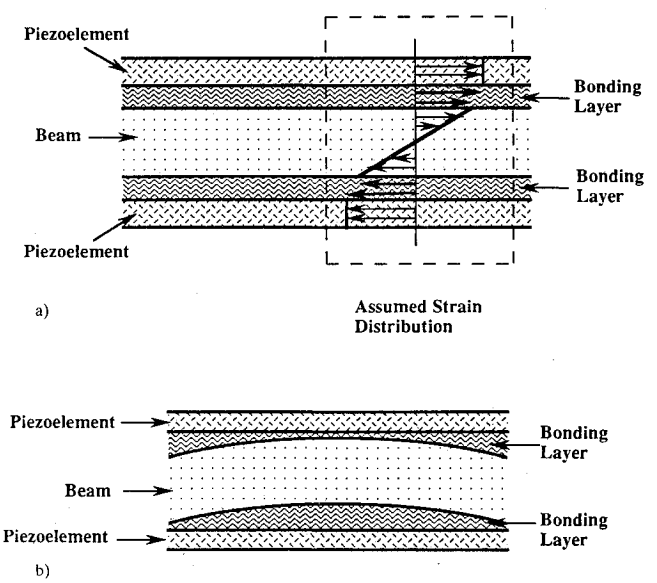

Fig. 1 Assumed strain distribution and deflection behavior of the composite structure of Crawley's study.[4] a) Assumed strain distribution; b) deflection behavior.

across the thickness direction, as shown in Fig. 3. Therefore, the strains at each of the interfaces will be continuous, and the centers for the radii of curvature for each layer should be concurrent.

Since the combined structure is assumed to be thin, plane stress theory can be applied. For the plate, the following stress-strain relationships can be derived[8]:

$$\sigma_{xp} = \frac{E_p}{1 - \nu_p^2}(\varepsilon_{xp} + \nu_p \varepsilon_{yp}) \tag{1}$$

$$\sigma_{yp} = \frac{E_p}{1 - \nu_p^2}(\varepsilon_{yp} + \nu_p \varepsilon_{xp}) \tag{2}$$

Here, the subscript p refers to the plate. Dimitriadis and Fuller[5] showed that strains in the x and y directions are equal for a homogeneous plate with a piezoactuator that gives equal free (unconstrained) strains in the x and y directions when it is activated. Consequently, stresses in x and y direction are also equal. Thus, the subscripts x and y will henceforth be omitted in stress-strain expressions giving only a single general stress-strain expression valid in both the x and y directions. Equations (1) and (2) then become:

$$\sigma_p = \frac{E_p}{1 - \nu_p} \varepsilon_p \tag{3}$$

Similarly, a stress-strain expression for the bonding layer can be expressed as:

$$\sigma_b = \frac{E_b}{1 - \nu_b} \varepsilon_b \tag{4}$$

Here, the subscript b refers to the bonding layer. In general, the assumption of linear strain across the bonding layer is not valid for thick bonding layers because of the viscoelastic nature of most epoxies. However, for piezoactuator applications, the bonding layer is generally comparatively thin (with respect to the substructure and piezoactuator). Thus, the linear strain assumption is approximately true.

The strain distribution is a linear function of z across the composite structure thickness in order to satisfy the prestated linear strain assumption. Therefore, the strain fields in each layer can be similarly expressed as a linear function of z as shown in Eq. (5):

$$\varepsilon(z) = \varepsilon_p = \varepsilon_b = \varepsilon_z = \Delta z \tag{5}$$

where Δ is the strain slope. Note that at the plate/bonding layer interface, the strains for each layer are identical so that strain continuity at the interface is guaranteed. However, because the material properties of the bonding layer (E_b and ν_b) are generally different from those of the plate, a discontinuity in the stress distribution at the plate/bonding layer interface occurs (see Fig. 3).

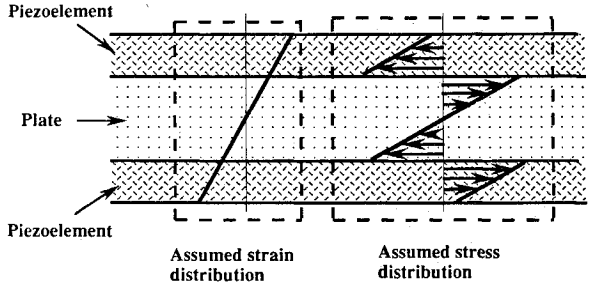

Fig. 2 Assumed stress and strain distribution of the composite structure of Dimitriadis's study.[5]

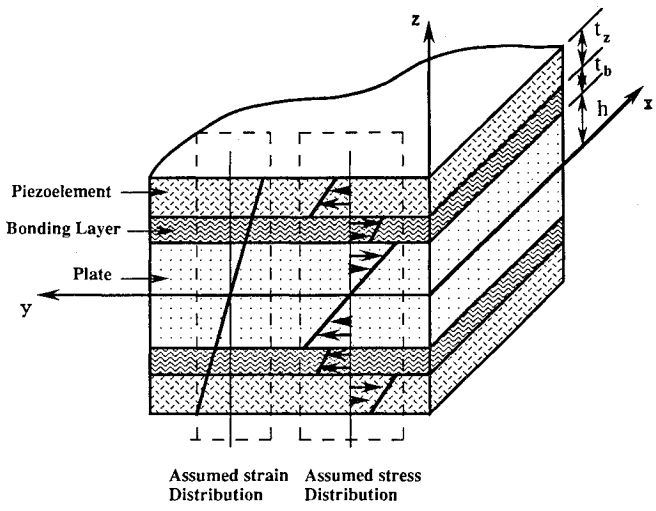

Fig. 3 Assumed stress and strain distribution of the composite structure of the current study.

Since a linear strain distribution was assumed across the plate thickness, the corresponding stress distribution can also be assumed to be linear, and can be expressed as a function of the interface stress of the plate $(\sigma_{il})_p$:

$$\sigma_p = \frac{(\sigma_{il})_p}{h} z \tag{6}$$

where h is the half-thickness of the plate. Using Eqs. (3), (5) and (6), the strain slope (Δ) can be obtained as a function of the interface stress of the plate $(\sigma_{il})_p$:

$$\Delta = \frac{1 - \nu_p}{E_p} \frac{(\sigma_{il})_p}{h} \tag{7}$$

From Eqs. (4), (5), and (7), the stress distribution in bonding layer then becomes:

$$\sigma_b = \frac{E_b}{1 - \nu_b} \Delta z = \frac{1 - \nu_p}{1 - \nu_b} \frac{E_b}{E_p} \frac{(\sigma_{il})_p}{h} z \tag{8}$$

Note that a stress discontinuity occurs at the plate/bonding layer interface since the plate and bonding layer in general have different material properties. Similarly, the stress slope of the bonding layer is also different from that of the plate (Fig. 3).

Generally, ferroelectric ceramics have five independent elastic material constants, and three independent piezoelectric constants.[7] When a voltage is applied in z direction, three normal strains can be induced. However, since the strain in the z direction cannot generate traction forces at the interface surfaces, its effect is neglected in this study. Furthermore, the frequency range under consideration in the active noise and vibration control area is much lower in comparison to the thickness resonance frequencies of the piezoactuator, which is typically over 1 MHz. Therefore, its effect can also be neglected in the dynamic behavior of composite structure. To simplify the problem, the ferroelectric ceramic piezoactuator is assumed to be elastically isotropic. From the linear piezoelectric constitutive equations, the stress-strain relationship for the piezoactuator can then be expressed as:

$$\sigma_z = \frac{E_z}{1 - \nu_z}(\varepsilon_z - \Lambda) \tag{9}$$

where

$$\Lambda = \frac{V}{t_z} d_{31} \tag{10}$$

Here, the subscript z refers to the piezoactuator. The variable Λ is the free piezoelectric strain and is a function of the applied voltage V, the piezoelectric strain constant d_{31}, and the piezoactuator thickness t_z. Therefore, as the thickness of the piezoactuator is reduced under a constant applied voltage, a higher free piezoelectric strain can be obtained.

From Eqs. (5), (7), and (9), the stress distribution in the piezoelectric patch becomes

$$\sigma_z = \frac{1 - \nu_p}{1 - \nu_z}\frac{E_z}{E_p}\frac{(\sigma_{il})_p}{h}z - \frac{E_z}{1 - \nu_z}\Lambda \tag{11}$$

Note again that a stress discontinuity occurs at the bonding layer/piezoactuator interface and that the stress slope is different from that of the plate and the bonding layer (Fig. 3). Since the free piezoelectric strain (Λ) is always greater than the restoring strain in the piezoactuator (ε_z), the direction of the piezoactuator stress is opposite of that in the plate and bonding layer, as shown in Fig. 3.

In Eqs. (6), (8), and (11), the stress relationship for the plate substructure, bonding layer, and the piezoactuator have each been expressed in terms of the unknown interface stress of the plate $(\sigma_{il})_p$. As the force equilibrium condition is automatically satisfied with the assumed stress distribution, the interface stress of the plate $(\sigma_{il})_p$ can be determined with the use of the moment equilibrium condition. Exploiting symmetry about the neutral axis, the moment equilibrium condition can be simplified as follows:

$$\int_0^h \sigma_p z\,dz + \int_h^{h+t_b} \sigma_b z\,dz + \int_{h+t_b}^{h+t_b+t_z} \sigma_z z\,dz = 0 \tag{12}$$

By applying Eq. (12), the interface stress of the plate $(\sigma_{il})_p$ is found to be:

$$(\sigma_{il})_p = \frac{3\gamma h t_z(2h + 2t_b + t_z)}{2[h^3 + \alpha t_b(3h^2 + 3ht_b + t_b^2) + \beta t_z(3h^2 + 3t_b^2 + t_z^2 + 6ht_b + 3ht_z + 3t_b t_z)]}\Lambda \tag{13}$$

where

$$\alpha = \frac{1 - \nu_p}{1 - \nu_b}\frac{E_b}{E_p}, \qquad \beta = \frac{1 - \nu_p}{1 - \nu_z}\frac{E_z}{E_p}, \qquad \gamma = \frac{E_z}{1 - \nu_z} \tag{14}$$

Here, the variables α and β represent nondimensional bonding layer and piezoactuator material property ratios, while γ is the piezoactuator stress-strain ratio.

The effective bending moment applied to the plate by the piezoactuator can then be expressed as a function of the known interface stress of the plate $(\sigma_{il})_p$, as

$$m_x = m_y = \int_{-h}^{h} \sigma_p z\,dz = \frac{2}{3}h^2(\sigma_{il})_p = \frac{\rho_z(2 + 2\rho_b + \rho_z)}{1 + \alpha\rho_b(3 + 3\rho_b + \rho_b^2) + \beta\rho_z(3 + 3\rho_b^2 + \rho_z^2 + 6\rho_b + 3\rho_z + 3\rho_b\rho_z)}h^2\gamma\Lambda \tag{15}$$

where

$$\rho_b = \frac{t_b}{h} \quad \text{and} \quad \rho_z = \frac{t_z}{h} \tag{16}$$

Here, ρ_b and ρ_z are the nondimensional thickness ratios of the bonding layer and piezoactuator, respectively. Thus, Eq. (15) is completely nondimensionalized with the exception of the far right term ($h^2\gamma\Lambda$). Also, note that the moment expression is given in terms of a line moment (N-m/m).

All of the above formulations are valid for a composite structure where the substructure (plate) is fully covered by the piezoactuators. However, in practice the piezoactuators only partially cover the plate. Consequently, free edges exist where the equilibrium condition requires that the normal stress at the actuator boundaries be zero, invalidating the above relationships. However, Liang and Rogers[9] showed that the actuator stress field for a distributed actuator is unaffected by the free edge except within approximately four actuator thicknesses of the boundary. Thus, for a large piezoactuator patch (with respect to the actuator thickness), the stress field is largely unaffected by the free boundaries. Consequently, the stress field described above in Eq. (13) generates a bending moment as described in Eq. (15), which is assumed to be uniform within the boundaries of the piezoactuator.

For the degenerate case of zero bonding layer ($\rho_b = 0$), Eq. (15) reduces to:

$$m_x = m_y = \frac{\rho_z(2 + \rho_z)}{1 + \beta\rho_z(3 + \rho_z^2 + 3\rho_z)}h^2\gamma\Lambda \tag{17}$$

In this case, the combined structure is essentially identical to that which Dimitriadis and Fuller investigated. The following equations, which are taken from Dimitriadis and Fuller[5] and cast into the nondimensional form as shown above, differ from the above equations only in that it was assumed that the plate and the piezoactuator had identical stress slopes across the thickness direction.

$$m_x = m_y = \frac{2\rho_z(2 + \rho_z)}{2 + 3\rho_z^2 + 2\rho_z^3 + 3\beta\rho_z(2 + \rho_z)}h^2\gamma\Lambda \tag{18}$$

Crawley and de Luis[4] have also shown that the finite piezoactuator perfectly bonded to a beam creates a uniform shear stress along the strip. The following equations are the effective moment expressions for a two-dimensional extension of this work:

$$m_x = m_y = \frac{2\rho_z}{\beta(\beta + 3\rho_z)}h^2\gamma\Lambda \tag{19}$$

This result again differs from the current work in the assumption of uniform strain across the piezoactuator.

Using classical thin-plate theory, the equation of motion of the plate with piezoactuator patches can be written as[5]

$$D_p\nabla^4 w + m''\ddot{w} = \frac{\partial^2 m_x}{\partial x^2} + \frac{\partial^2 m_y}{\partial y^2} \tag{20}$$

where w is the transverse displacement, D_p is the plate flexural rigidity, and m'' is the area mass density of the plate. Note

that the effective bending moments from the piezoactuator patches can be interpreted as the external plate loads.

Results and Discussion

The final expression for the effective bending moment is a function of the thickness and the material properties of the plate, the bonding layer, and the piezoactuator. The bending moment also depends on the free piezoelectric strain Λ. As shown in Eq. (10), the free piezoelectric strain is proportional to applied electric field (V/t_z). The proportionality constant d_{31} is the piezoelectric strain constant and represents the degree of electromechanical coupling of the piezoelectric material. From Eqs. (10) and (15), it is clear that the effective moment is directly proportional to the piezoelectric strain constant. Thus, to maximize the applied bending moment, a material with a high piezoelectric strain constant is desirable. However, the value of the piezoelectric strain constant acts just as a multiplying factor and has no bearing on the optimal thickness of the piezoactuator.

From Eqs. (10) and (15), it is also apparent that theoretically much greater moments can be expected with thinner piezoactuators under a constant applied voltage. However, this observation leads to the spurious conclusion that the thinner the piezoactuator, the better. In practice, piezoelectric materials have a maximum allowable electric field strength that is less than V/mm for most commercially available piezoelectric materials. If the maximum allowable field strength is exceeded, the material will degrade and eventually lose its piezoelectric properties. Thus, in optimizing the piezoactuator thickness, the electric field strength (V/t_z) should be held constant rather than the applied voltage (V) to correctly represent the true nature of piezoelectric materials. Furthermore, since most piezoactuators do not require much electric current for operation, power amplifiers capable of providing the high voltages needed for thicker piezoactuators can be devised relatively easily. In such cases, the optimal thickness of piezoactuators under constant electric field may provide valuable information for practical implementation. An analogy can be found between the optimal thickness of piezoactuators and the optimal thickness of bimetal composite structures of which the driving forces are derived from thermal strains.

In this study, the plate under question is assumed to be steel while the bonding layer is assumed to be epoxy. Also, the piezoactuators are assumed to be of piezoceramic materials. The material properties and thicknesses of the aforementioned components under discussion are shown in Tables 1 and 2.

Comparison of Effective Moment

A comparison of the effective moment induced by a piezoactuator, assuming a bonding layer thickness of zero (perfect bonding, $\rho_b = 0$), from the current and previous studies, is shown in Fig. 4. The applied electric field strength is assumed to be 100 V/mm, which approaches the maximum allowable electric field strength for most piezoelectric ceramic materials in continuous use. Therefore, the free piezoelectric strain Λ becomes 2.0×10^{-5} mm/mm by use of the piezoelectric strain constant in Table 1. In this figure, the effective moment is given as a line moment with units of N-m/m and is a function of the nondimensional piezoactuator thickness ($\rho_z = t_z/h$), based on the half-plate thickness (h). The present results are in good agreement with those of Crawley and de Luis for piezoactuators with thicknesses up to a quarter-plate thickness ($h/2$). However, a noticeable discrepancy is observed as the piezoactuator thickness is increased beyond a quarter-plate thickness. Since Crawley and de Luis[4] assumed uniform strain across the piezoactuator layer, their theory becomes invalid for thicker piezoactuators, thus accounting for the discrepancy shown in Fig. 4. Essentially, the uniform strain assumption causes a underprediction of the restoring stress in the piezoactuator as its thickness is increased. Consequently, an overestimation of the effective moment results.

It is also seen that noticeable discrepancies exist between results of Dimitriadis[5] and this study. These discrepancies can likewise be reconciled by noting the different piezoactuator stress slope assumption utilized in their study, as discussed previously. This assumption has the effect of overestimating the restoring stress in the piezoactuator, thus resulting in an underestimation of the effective moment.

Table 1 Elastical properties of materials

	$E/10^{11}$, N/m^2	ν	t, mm
Steel plate	2.07	0.292	2
Aluminum plate	0.71	0.33	2
Epoxy bond[a]	0.021	0.4	0.1[a]

[a]Nominal value.

Table 2 Typical piezoelectric material properties

	$d_{31}/10^{-12}$, m/V	$E/10^{11}$, N/m^2	ν	E_f, V/mm
Piezoceramic	200	0.65	0.3	200

Optimal Thickness of Piezoactuator

In Fig. 4, it is shown that the effective moment goes to zero when the piezoactuator thickness (t_z) approaches zero. This limiting case represents the trivial situation of infinitely thin piezoactuator resulting in an infinitely small applied moment. The effective moment again approaches zero when the piezoactuator thickness becomes large because the flexural rigidity of the piezoactuators limit the bending strain. Consequently, the interface stress of the plate becomes small, reducing the effective moment. Therefore, there must exist a nonzero value of the effective moment between the limiting cases, which maximizes the effective moment.

Figure 4 shows that the optimal thickness for the piezoactuator approaches the half-plate thickness, $\rho_z \sim 1$ (assuming a steel plate). Therefore, the combined structure with the optimal piezoactuator can generally still be considered thin in comparison to the in-plane plate dimensions so that the stated assumptions of plane stress theory and the linear strain remain valid. For the properties chosen in Fig. 4, the maximum effective bending moment is approximately 2 N-m/m. It is important to note that if the optimal thickness is not available, then it is generally better to choose a slightly thicker piezoactuator than a slightly thinner one because the decrease in the effective moment is less severe.

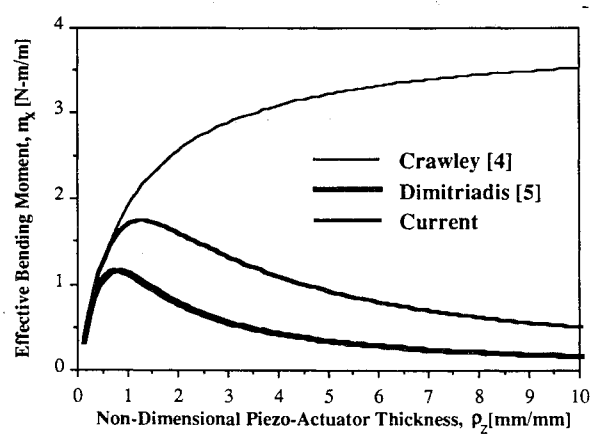

Fig. 4 A comparison of the effective bending moment induced by a pair of surface-bonded piezoactuators from the current and preexisting methods ($E_p = 2.07 \times 10^{11}$, $E_z/E_p = 0.314$, $\nu_p = 0.292$, $\nu_z = 0.3$, $h = 1$, $t_b = 0$, $\Lambda = 2.0 \times 10^{-5}$).

In Fig. 5, the effective bending moment, again assuming a bonding layer thickness of zero, is shown as a function of the nondimensional piezoactuator thickness and Young's modulus ratios of the piezoactuator (i.e., ρ_z and E_z/E_p, respectively). In this figure, a family of moment curves is presented for a range of piezoactuator Young's modulus ratios (E_z/E_p). Note that the nominal value of the Young's modulus ratio for commercially available piezoactuators is about 0.3, assuming a steel plate. Higher bending moments are induced with stiffer piezoactuators, which is in agreement with the previous studies.[3] However, there exists a maximum limiting value which can be obtained by increase the Young's modulus of the piezoactuator. As E_z/E_p approaches infinity, the effective moment approaches a limiting value of

$$m_x = m_y = \frac{2 + \rho_z}{3 + 3\rho_z + \rho_z^2} \frac{E_p}{1 - \nu_p} h^2 \Lambda \qquad (21)$$

Therefore, the effective moment cannot have an arbitrarily high value by stiffening the piezoactuator. In addition, the optimal thickness of the piezoactuator decreases with stiffer piezoactuators. Note also that as the piezoactuator Young's modulus ratio (E_z/E_p) increases, the penalty for deviating from the optimal thickness increases since the effective moment curve becomes sharp.

Effects of Bonding Layer

In order to investigate the effect of the bonding layer thickness, another family of moment curves is presented in Fig. 6 as a function of the nondimensional bonding layer thickness (ρ_b). Thicker bonding layers give moderately lower bending moments. However, the optimal actuator thickness does not seem to be significantly affected by the bonding layer thickness so long as reasonable values are used.

As discussed in the analysis, the assumption of linear strain across the bonding layer is valid only for thin bonding layers ($\rho_b \ll 1$). These results are useful because they give an upper bound to the effective bending moment for increasing bonding layer thickness. In practice, the influence of the bonding layer thickness will be more significant, especially for thicker bonding layers as shown in Fig. 6. Nevertheless, this result clearly illustrates the benefit of thin bonding layers.

Figure 7 shows the effect of the bonding layer Young's modulus ratio on the effective moment. Interestingly, stiffer bonding layers tend to give lower bending moments, which is in agreement with previous studies.[4] However, the influence of the bonding layer Young's modulus ratio is insignificant because a typical value of the ratio is approximately 0.01, which is two orders of magnitude below the piezoactuator

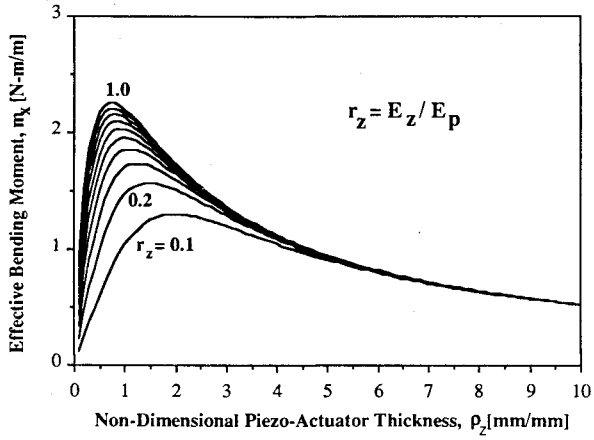

Fig. 5 Effective moment curves illustrating the influence of the piezoactuator Young's modulus on the optimal piezoactuator thickness (E_p = 2.07 × 10^{11}, ν_p = 0.292, ν_z = 0.3, h = 1, t_b = 0, Λ = 2.0 × 10^{-5}).

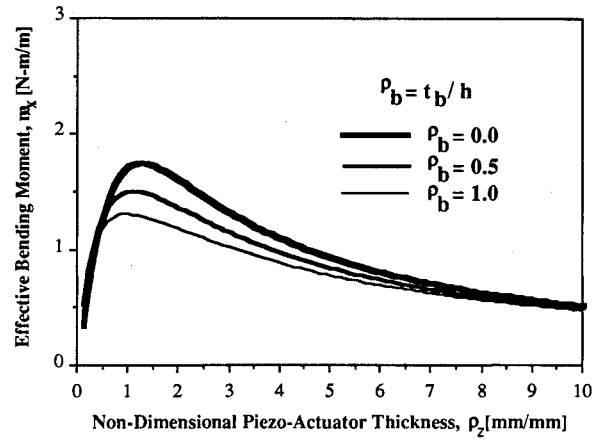

Fig. 6 Effective moment curves illustrating the influence of the bonding layer thickness on the optimal piezoactuator thickness (E_p = 2.07 × 10^{11}, E_z/E_p = 0.314, E_b/E_p = 0.01, ν_p = 0.292, ν_z = 0.3, ν_b = 0.4, h = 1, Λ = 2 × 10^{-5}).

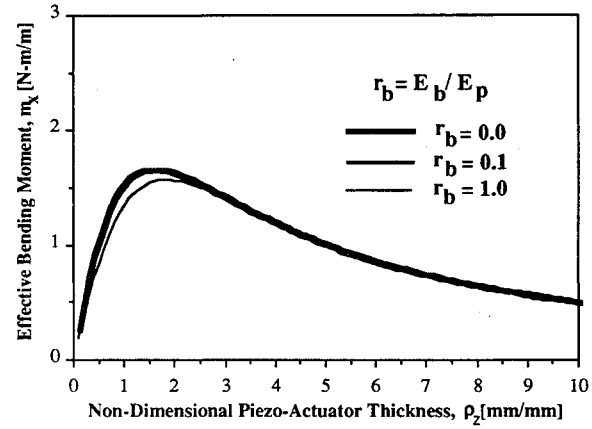

Fig. 7 Effective moment curves illustrating the influence of the bonding layer Young's modulus on the optimal piezoactuator thickness (E_p = 2.07 × 10^{11}, E_z/E_p = 0.314, ν_p = 0.292, ν_z = 0.3, ν_b = 0.4, h = 2, t_b = 0.1, Λ = 2.0 × 10^{-5}).

Young's modulus ratio. Nevertheless, the effect of stiffening the bonding layer is effectively equivalent to stiffening the plate, thus reducing the applied bending moment.

The effects of damping (η) and Poisson's ratio (ν_b) of the bonding layer were also investigated. Damping was introduced by making Young's modulus of the bonding layer complex [i.e., $E_b^c = E_b(1 + j\eta)$]. As shown in Fig. 8 the effect of damping is insignificant even for unrealistically high values of damping. Similarly, the effect of Poisson's ratio is also insignificant, and thus is not shown.

Effects of Elastic Substructure

All of the above discussions are with respect to a steel substructure. However, aluminum is another commonly used material for structures such as aircraft and rotorcraft. Therefore, the effective moment is also investigated for an aluminum substructure. A comparison of the effective moment for the aluminum plate with that for the steel plate is shown in Fig. 9. Note that the effective moment for the aluminum plate is significantly smaller than that of the steel plate. This is because Young's modulus of aluminum is smaller than that of the steel. However, the actual vibration induced by the piezoactuators depends on the ratio of the effective moment to the flexural rigidity. As shown in Fig. 10, since the flexural rigidity of the aluminum plate is approximately one-third of that of the plate, the induced vibration is slightly higher for the aluminum substructure. Also, the optimal thickness approaches a quarter-plate thickness for the aluminum substructure. Thus, the optimal thickness of the piezoactuator is also

dependent on the substructure material properties. Consequently, the piezoactuator thickness should be reoptimized for differing substructures.

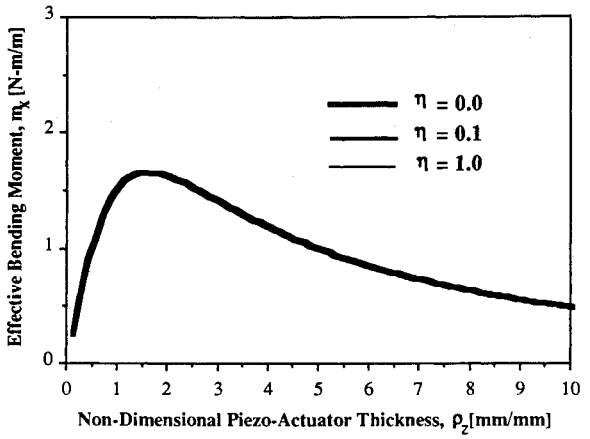

Fig. 8 Effective moment curves illustrating the influence of the damping of the bonding layer on the optimal piezoactuator thickness (E_p = 2.07 × 10^{11}, E_z/E_p = 0.314, E_b/E_p = 0.01, ν_p = 0.292, ν_z = 0.3, ν_b = 0.4, h = 1, t_b = 0.1, Λ = 2.0 × 10^{-5}).

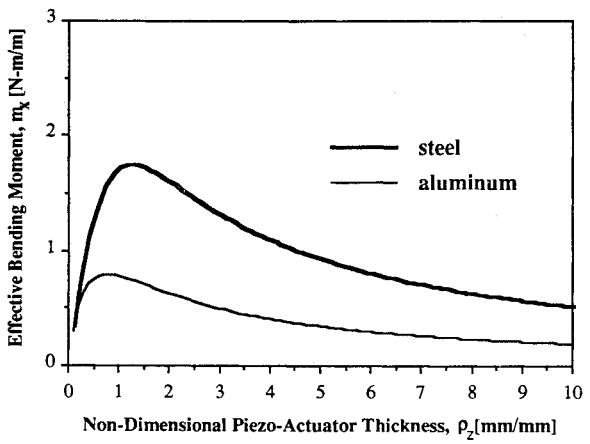

Fig. 9 Effective moment curves illustrating the influence of the substructure on the optimal piezoactuator thickness. (Data given in Table 1 were used; no bonding layer.)

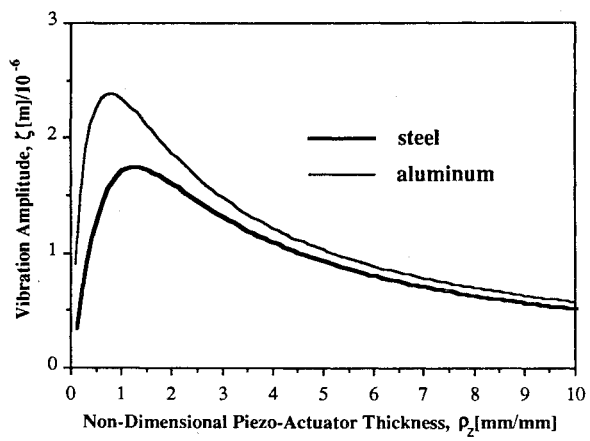

Fig. 10 Expecting vibration amplitudes induced by the piezoactuators in Fig. 9.

Conclusions

A new expression is derived for the effective bending moment induced by a pair of surface-bonded piezoactuators to an elastic substructure (plate) under the assumption of thin composite plates. Comparisons between this study and previous investigations showed that noticeable discrepancies exist. These discrepancies are explained by the different assumptions made in the individual studies.

This study has shown that, for commercially available piezoactuators and bonding materials, there exists an optimal thickness of the piezoactuator that maximizes the bending moments under a constant applied electric field. It was also demonstrated that the optimal thickness for commercially available piezoactuators is approximately a half-plate thickness for a steel substructure and a quarter-plate thickness for an aluminum substructure. The optimal thickness of the piezoactuators is affected by their Young's modulus, becoming thinner with stiffer piezoactuators. In addition, stiffer piezoactuators provide higher bending moments. Furthermore, it has also been shown that the most important factor of the bonding layer is its thickness. The effective bending moments induced by the piezoactuators increase with a diminishing bonding layer thickness without significant affect on the optimal piezoactuator thickness. In contrast, the influence of Young's modulus, Poisson's ratio, and the damping of the bonding layer are not important factors in optimizing the piezoactuator/substructure coupling, given the bonding layer is thin with respect to the composite thickness.

Acknowledgments

The authors gratefully acknowledge the support of this work by the National Science Foundation under NSF-Presidential Young Investigator Grant MSS-8957191. The authors also appreciate the financial contributions of GoldStar Co., Ltd., in Korea, whose funding supports the doctoral studies of Sung Jin Kim. Finally, the authors thank Peter Chang for his efforts in helping prepare this manuscript.

References

[1]Bailey, T., and Hubbard, J. E., "Distributed Piezoelectric-Polymer Active Vibration Control of a Cantilever Beam," *Journal of Guidance, Control, and Dynamics*, Vol. 8, No. 5, 1985, pp. 605–611.

[2]Fansen, J. L., and Chen, J. C., "Structural Control by the Use of Piezoelectric Active Members," *Proceedings of NASA/DOD Control-Structures Interaction Conference*, NASA CP-2447, Part II, 1986.

[3]Baz, A., and Poh, S., "Optimum Vibration Control of Flexible Beams by Piezoelectric Actuators," NASA CR-180209, 1987.

[4]Crawley, E. F., and de Luis, J., "Use of Piezoelectric Actuators as Elements of Intelligent Structures," *AIAA Journal*, Vol. 25, No. 10, 1987, pp. 1373–1385.

[5]Dimitriadis, E. K., and Fuller, C. R., "Piezoelectric Actuators for Noise and Vibration Control of Thin Plates," 12th ASME Conference on Mechanical Vibration and Noise, Montreal, 1989.

[6]Dimitriadis, E. K., and Fuller, C. R., "Investigation on Active Control of Sound Transmission Through Elastic Plates Using Piezoelectric Actuators," AIAA Paper 89-1062, AIAA 12th Aeroacoustics Conference, San Antonio, TX, April, 1989.

[7]Tiersten, H. J., *Linear Piezoelectric Plate Vibration*, Plenum Press, New York, 1969, pp. 54–55.

[8]Fung, Y. C., *Foundations of Solid Mechanics*, Prentice-Hall, Englewood Cliffs, NJ, 1965, pp. 233–234.

[9]Liang, C., and Roger, C. A., "Behavior of Shape Memory Alloy Actuators Embedded in Composites," *Proceedings of the 1989 International Composite Conference*, Beijing, China, Aug. 1989.